Journal of the Earth and Space Physics, Vol. 41, No. 4, 2016, PP. 13-22

Moment tensor and stress inversion for an active fault system in west part of Lut-Block, Iran

Ataei, N.[1] and Rezapour, M.[2*]

1. M.Sc. Student, Department of Earth Physics, Institute of Geophysics, University of Tehran, Iran
2. Associate Professor, Department of Earth Physics, Institute of Geophysics, University of Tehran, Iran

(Received: 16 Jun. 2014, Accepted: 23 Sep. 2014)

Abstract

Iran is one of the most tectonically active regions on the Alpine-Himalayan earthquake belt. Eastern Iran, nowadays, is one of the most active regions of the country. The occurrence of several destructive earthquakes during the past 50 years provides the evidence for the seismic activity in this region. The earthquakes are mostly concentrated around the Lut-block. There are strike-slip fault systems with nearly north-south strike, east and west of the Lut-block. The fault system located in the west part of the Lut-block includes Tabas, Nayband, Lakarkuh, Gowk and Sabzevaran faults. This system is of great importance since it has generated destructive earthquakes such as Dasht-e-Bayaz. Since understanding the focal mechanism of the fault responsible for earthquake is one of the most important parameters, the accuracy to calculate the focal mechanism is extremely vital. Therefore, we have calculated focal mechanisms of the 34 recent earthquakes happened on this system using full moment tensor inversion. The waveform data from 8 broad-band stations, operated by International Institute of Earthquake Engineering and Seismology (IIEES), was used in this study. Appling ISOLated Asperities (ISOLA) package for the full moment tensor inversion using the local and regional data enables us to achieve a higher accuracy in determined focal mechanisms, in comparison with other methods which use teleseismic data. As the magnitude of these events are all smaller than 5.5 (the biggest one equals 5.2), it was not possible to obtain the focal mechanism of almost all of these events through CMT solutions using teleseismic data. The obtained focal mechanisms show that the main mechanism of the Nayband-Gowk-Sabzevaran system is right-lateral strike-slip with a reverse component. The trends of the three main stress axes were also calculated using the 32 focal mechanisms and the stress inversion technique. The results show that the second stress axis (σ_2) is nearly vertical, which is one of the characteristics of the strike-slip regimes.

Key words: Focal mechanism, ISOLA, Moment tensor inversion, Stress inversion, Strike-slip faulting.

1. Introduction

The active deformation of Iranian plateau is attributed to Arabian-Eurasian convergence. Continental Shortening is being moderated by faulting and folding, mostly within the high mountain ranges in the south-southwest (Zagros) and the north-northeast (Alborz and Kopeh Dagh) areas of Iran. The amount of shortening which cannot be taken up in these areas must be expressed in the eastern region as a strike-slip shear. This shear is manifested on both the west and east sides of the Dasht-e-Lut. Dasht-e-Lut, located in East Iran, near the Iran-Afghanistan border, is a flat aseismic rigid block. This block is surrounded by two North-South fault systems at either side (Walker and Jackson, 2002; Walker et al., 2004; Berberian et al., 2001). In this paper we focused on the Nayband-Gowk fault system (Fig. 1). Several destructive earthquakes have happened on this system since the 1979 Tabas earthquake. For example, the northern part of the Gowk fault ruptured five times from 1981 to 1998. Nevertheless, the southern part remains as a potential seismic source in this region. A large number of researches have been done on this region. 34 earthquakes ($Mw > 4$) happened on this fault system from 2004 to 2012 (Table 1). Data for two of them were of such poor quality that made the analysis of the seismogram

*Corresponding author: E-mail: rezapour@ut.ac.ir

impossible. The other 32 were analyzed in this study using seismic moment tensor inversion with ISOLA (ISOLated Asperity) software. As these events are all small in magnitude ($M_L \leq 5.2$), the CMT solution for just two of these events has been stated by Harvard CMT, which is shown in Table 4 in gray. Afterwards, the focal mechanisms of these 32 earthquakes were used in order to calculate the principal stress axes in the region of the study by means of stress inversion. Eight broad-band stations of the International Institute of Earthquake Engineering and Seismology (IIEES) within the regional distance were used (Table 2). As these events were not destructive or big enough, the focal mechanism in most of them had not been determined before this study by any seismological center. However, for the few available on Harvard CMT the comparison has been done. To model a waveform, it is possible to use the whole or a part of the waveform, i.e., body waves, surface waves or both of them (Zahradnik et al., 2001; Dziewonski, 1981; Kanamori and Given, 1981; Sterlitz, 1978). Precise knowledge of source parameters (scalar moment, strike, dip and rake) helps us understand the physical process on the faults which had generated the earthquakes. Although some information can be extracted from the first few seconds of the seismic records (such as location, fault plane solution, etc.), to go further, detailed studies of the complete seismogram are necessary. These studies can provide further constraints on the hypocentral depth and earthquake moment, providing valuable information on a region's deformation style (Sokos and Zahradnik, 2008).

In this study, the focal mechanisms were determined by modeling the whole waveform using ISOLA software. At first, we will introduce the method being used and the advantages of this method in comparison with other ones. Then, the analysis of the seismological data and the output will be presented. Finally, the three principal stress axes will be derived using bootstrap stress inversion.

2. Data

The reported parameters by IIEES for 34 selected earthquakes are listed in Table 1. Table 2 shows the coordinates of the seismic stations used in this study. The earth model being used has been shown in Table 3.

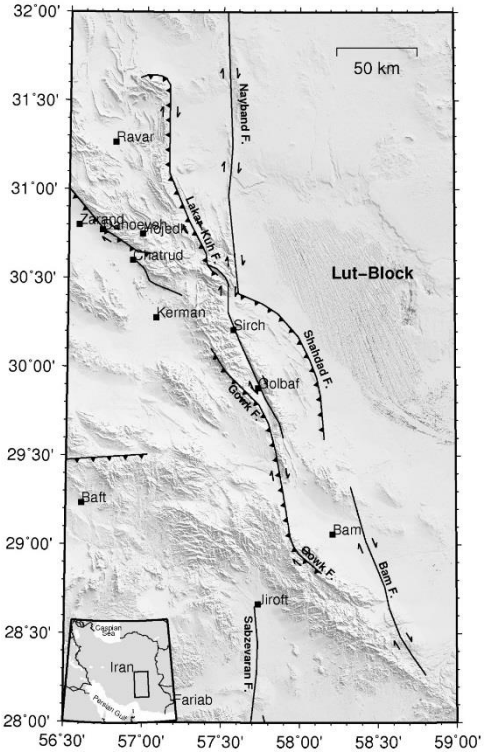

Fig. 1. The map of the study area that shows the major active faults in the west part of Lut-Block. The squares indicate the location of the cities. The solid lines show traces of active faults in the region (Hessami et al., 2003).

Table 1. The parameters of 34 earthquakes included in this study

No.	Date (y/m/d)	Origin Time (UTC)	Lat (N°)	Long (E°)	Depth (km)	Magnitude (M_L)
1	2004/10/06	11:14:26.1	28.83	57.93	14	5.2
2	2004/10/07	07:16:59.9	28.84	57.96	14	4.3
3	2004/10/08	07:15:57.1	29.25	58.42	14	4.1
4	2004/10/14	02:28:42.9	31.73	57.05	18	5.1
5	2004/10/14	06:18:38.3	31.71	57.18	18	4.2
6	2004/12/23	11:01:10.3	28.53	57.07	14	4
7	2005/01/10	18:38:28.1	28.68	57.86	14	4
8	2005/01/30	08:30:51.6	29.28	58.46	14	4.3
9	2005/05/01	18:58:38.8	30.80	57	14	5.1
10	2005/09/05	14:12:31.4	28.59	58.34	15	4.2
11	2005/12/27	16:13:47.6	30.08	57.76	14	4
12	2006/02/06	19:58:18.6	29.30	58.43	14	4.1
13	2006/02/06	23:31:55.3	29.35	58.44	14	4.2
14	2006/06/04	16:18:27.1	30.41	57.33	14	4.3
15	2006/08/31	02:28:30.2	30.27	57.44	15	4
16	2006/10/25	10:04:00.7	28.61	57.08	16	4
17	2006/12/09	08:09:08.1	28.64	58.11	14	4.3
18	2006/12/13	13:32:05.5	30.52	57.58	14	4.4
19	2007/03/26	06:36:50.0	29.17	58.45	14	5
20	2007/12/25	15:34:52.9	29.16	58.09	14	4
21	2008/05/27	17:07:21.5	30.49	57.08	14	4
22	2008/06/21	16:21:17.7	30.41	57.55	14	4.1
23	2008/06/23	07:14:52.3	29.24	58.24	15	4
24	2009/02/15	21:22:19.2	31.06	57	18	4.6
25	2009/05/11	02:14:05.1	30.29	57.50	18	4.7
26	2009/06/24	20:50:22.0	29.96	57.71	18	4
27	2009/10/17	17:08:08.8	30.18	57.44	12	4.1
28	2010/01/05	18:54:43.6	29.09	58.48	14	4.1
29	2010/01/26	03:17:00.5	30.82	57.10	14	4.2
30	2010/02/03	22:39:45.2	28.59	57.01	14	4.3
31	2011/01/09	18:11:04.4	30.33	57.33	14	4.5
32	2011/06/26	19:46:58.6	30.12	57.54	16	5.1
33	2012/04/29	11:58:38.4	28.58	57.40	31	4.2
34	2012/09/21	03:28:30.0	31.95	58.31	14	4.8

Table 2. The coordinates of the 6 broadband IIEES stations.

Station name	Code	Lat. (N°)	Long. (E°)	Elevation (m)
Kerman	**KRB**	**29.98**	**56.76**	**2576**
Zahedan	**ZHS**	**29.61**	**60.78**	**1575**
Bandar Abbas	**BND**	**27.40**	**56.17**	**1500**
Ghir-Karzin	**GHI**	**28.29**	**52.99**	**1200**
Naeen	**NAS**	**32.80**	**52.81**	**2379**
Chabahar	**CHB**	**25.60**	**60.48**	**125**
Shahrakht	**SHT**	**33.65**	**60.29**	**837**
Tabas	**TAB**	**33.65**	**57.12**	**1106**

Table 3. The adopted earth model of Iran used in IIEES.

Depth(km)	Vp(km/s)	Vs(km/s)	Density(g/cm^3)
0	**5.40**	**3.034**	**2.780**
6	**5.90**	**3.315**	**2.880**
14	**6.30**	**3.539**	**2.960**
18	**6.50**	**3.652**	**3.000**
46	**8.05**	**4.522**	**3.310**
72	**8.10**	**4.551**	**3.320**

We process three component seismograms recorded by 8 broad-band stations (Guralp CMG-3T-360s and CMG-3ESP-120ssensors) from Iranian National Seismic Network (INSN) deployed in the Iranian Plateau by IIEES. Our dataset consists of seismograms with a good signal-to-noise ratio from the events with M_L magnitude between 4.0 and 5.2.

3. Seismic moment and stress inversion

In this study, ISOLA software was used to perform the full waveform inversion. This method was first used to determine the source parameters at teleseismic distances (Kikuchi and Kanamori, 1991). Zahradnik et al. (2005) developed this method for regional and local distances by calculating the Green's functions using discrete wave number method (Bouchon, 1981). Full waveform of regional data (station distances vary from ~100 to ~700 km) was used for linear inversion of the moment tensor in the time domain. In this method, the velocity records are improved by using a mid-band filter, after applying instrumental correction on them. The velocity records are converted into displacement data; then the linear inversion in time domain is being done by calculating the Green's functions for the displacement data on each station to determine the calculated displacement. Finally, the inversion process is done through the linear composition of fundamental seismograms and the six moment tensor components. The fundamental seismograms are related to the six fundamental focal mechanisms (Kikuchi and Kanamori, 1991). Therefore, the three-component seismograms are obtained from the data while the moment tensor components are the unknown parameters. The moment tensor eigenvectors give the amount of scalar moment (M_0), strike, dip, and rake. It also illustrates the DC (double-couple) percentage of the moment tensor. Despite the quantities of M_0, strike, dip, and rake, the amount of the DC% is unstable. The reason is that a divergence in the shear mechanism has a slight effect on the seismograms. Consequently, typically the DC% doesn't have a physical interpretation

(Zahradnik et al., 2008). That is why we generally count on the variance reduction value which shows the correlation between the observed and synthetic values. The value of the condition number was also considered for a better interpretation. In this method, it is assumed that the location and time of the source is known. ISOLA will also optimize these values by grid searching. The grid search goes on until the points with the minimum least-square errors are found; this is equal to the maximum correlation of the observed and synthetic seismograms. If the earthquake is assumed as a single-event, then the best fit from the grid search is the location of the centroid (Zahradnik et al., 2008). We determined the source parameters of 34 events by waveform modeling. As an example, the correlation between the synthetic and observed seismograms and moment tensor solution for event number 32 are shown in Figures 2 and 3, respectively.

The stress field in a region can be calculated using tangential traction on several faults (Michael, 1984; Bott, 1959). To do this, the stress field tensor should be assumed as a fixed tensor during the time of the earthquakes in the region (Michael, 1984). Therefore, in stress inversion the aim is to find the stress tensor caused the faulting. To perform stress inversion in the slip data, the fault plane should be known. In this study, only the focal mechanism data are available. To determine the stress tensor by means of focal mechanism, we used a statistical tool named bootstrap re-sampling. In this method, each plane is considered to be the fault plane and the one fitting the stress tensor the best, would be picked as the main plane. In the end, the stress tensor can match a number of planes so that the best is considered the stress tensor (Michael, 1987).

4. Results

As mentioned before, in this project, the data were obtained from eight broad-band three-component stations of the International Institute of Earthquake Engineering and Seismology (IIEES) (for some earthquakes the number of stations were less). The results from the waveform inversions are shown in Table 4. The Harvard CMT solution is available only for two events, numbered 1 and 32. In Table 4, we put the CMT solution for these events under the determined parameters in this study. The focal mechanisms have been all derived from deviatoric moment tensors as the retrieval of the volumetric part is problematic and it doesn't play an important role in tectonic earthquakes. Also the DC constraint makes the inversion nonlinear and the parameters coming from the deviatoric inversion are close to those from the DC-constrained inversion because the amounts of strike, dip, and rake are robust (Zahradnik et al., 2008; Henry et al., 2002).

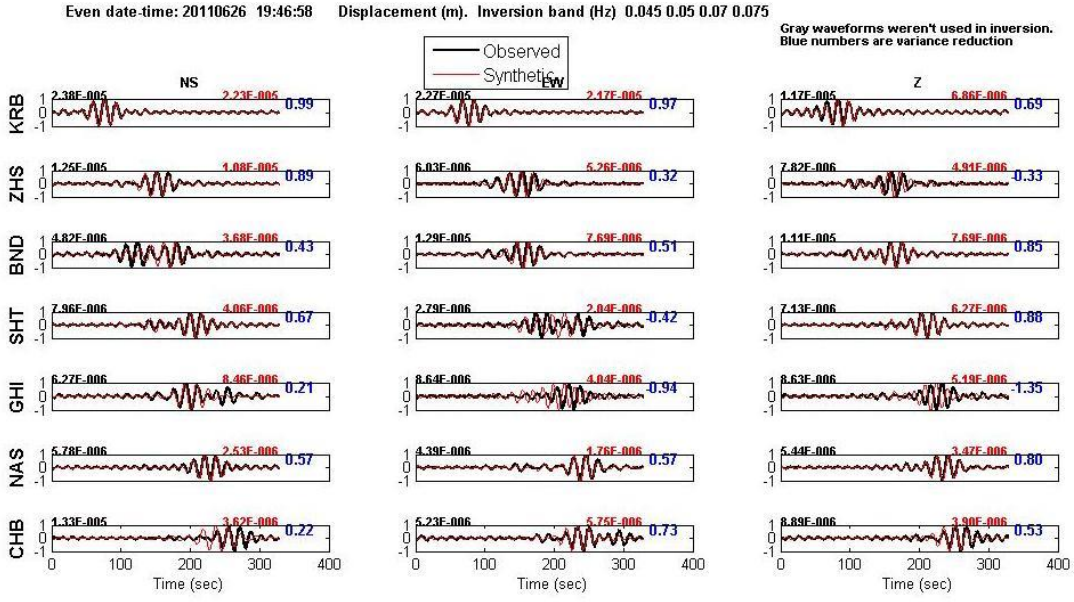

Fig. 2. The figure illustrates the correlations between the synthetic and observed seismograms for the 32nd event observed in 7 stations. The numbers on the top left and top right represent peak amplitude of the observed and synthetic waves, respectively.

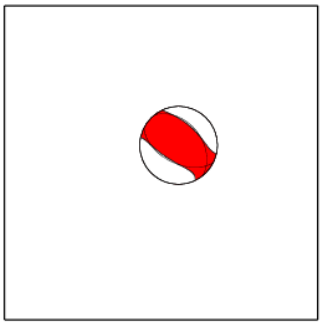

MOMENT TENSOR SOLUTION

HYPOCENTER LOCATION (IIEES)

Origin time 20110626 19:46:58.60
Lat 30.12 Lon 57.54 Depth 16

CENTROID

Trial source number : 19 (Multiple Source line or plane inversion)
Centroid Lat 30.129 Lon 57.5504
Centroid Depth : 14
Centroid time : +1.4 (sec) relative to origin time

Moment (Nm) : 3.389e+016
Mw : 5
DC% :56.6
CLVD% :43.4
Var.red.(for stations used in inversion):0.62
Var.red.(for all stations) :0.62

Strike	Dip	Rake
321	41	109
Strike	**Dip**	**Rake**
117	52	74

P-axis	Azimuth	Plunge
	218	6
T-axis	**Azimuth**	**Plunge**
	333	76

Mrr	Mtt	Mpp
2.745	-1.895	-0.850
Mrt	**Mrp**	**Mtp**
0.798	-0.060	2.218

Exponent (Nm): 16

Stations-Components Used			
Station	NS	EW	Ver
KRB	+	+	+
ZHS	+	+	+
BND	+	+	+
SHT	+	+	+
GHI	+	+	+
NAS	+	+	+
CHB	+	+	+

Fig. 3. The calculated moment tensor for the 32nd event calculated by the ISOLA software

Variance reduction shows how well a synthetic seismogram matches the observed one; as a result, this shows a perfect match. In reality, this is not possible (because of the incompleteness in crustal models, the uncertainty in earthquake locations).

However, the more the number approximates one, the better it would be matched.

Another factor that shows the reliability in the result of an inversion has been shown in the 9th column. If the inverse of the condition number (system's eigenvalue) is near or more than 0.1, we can conclude that the inversion is reliable (Zahradnik et al., 2008). More important than all of these is the focal mechanism stability. To see how stable a focal mechanism is, the moment tensor inversion was performed several times in different frequency ranges between 0.01-0.1 for each event.

Figure 4 shows the focal mechanisms of the 32 calculated earthquakes with their optimized locations. As it is clear in the figure, the predominant focal mechanism on the Nayband-Gowk-Sabzevaran fault system is strike-slip and reverse. There are some normal mechanisms as well. These mechanisms are probably related to the pull-apart basins created in the area, not dominant though. Something else that is worth mentioning is the absence of moderate-sized earthquakes (studied here) in the southern part of the Gowk fault. As a result, this part of the fault will remain potential for the next destructive earthquake in this area.

5. The principal stress axes

In order to calculate the three principal stress axes, bootstrap re-sampling technique was used in this research. Based on the data we had access to (the focal mechanism, not the fault plane), the bootstrap technique seemed to be the best method, as it is not essential to know which nodal plane is the fault plane (Michael, 1987).

The re-sampling of the 32 focal mechanisms with bootstrap technique is shown in figure 5a. In figure 5b the final result is shown on a stereonet. The trend values related to the three main principal axes (σ_1, σ_2 andσ_3) in the region of study are 213.7, 343.5 and 122.1 degrees, respectively. The plunge values are 8.3, 77.2 and 9.6 degrees. As it is obvious the σ_2 axis is nearly vertical, while the other two (σ_1, σ_3) are nearly horizontal. This result is in line with this region's tectonic (mainly strike-slip shear).

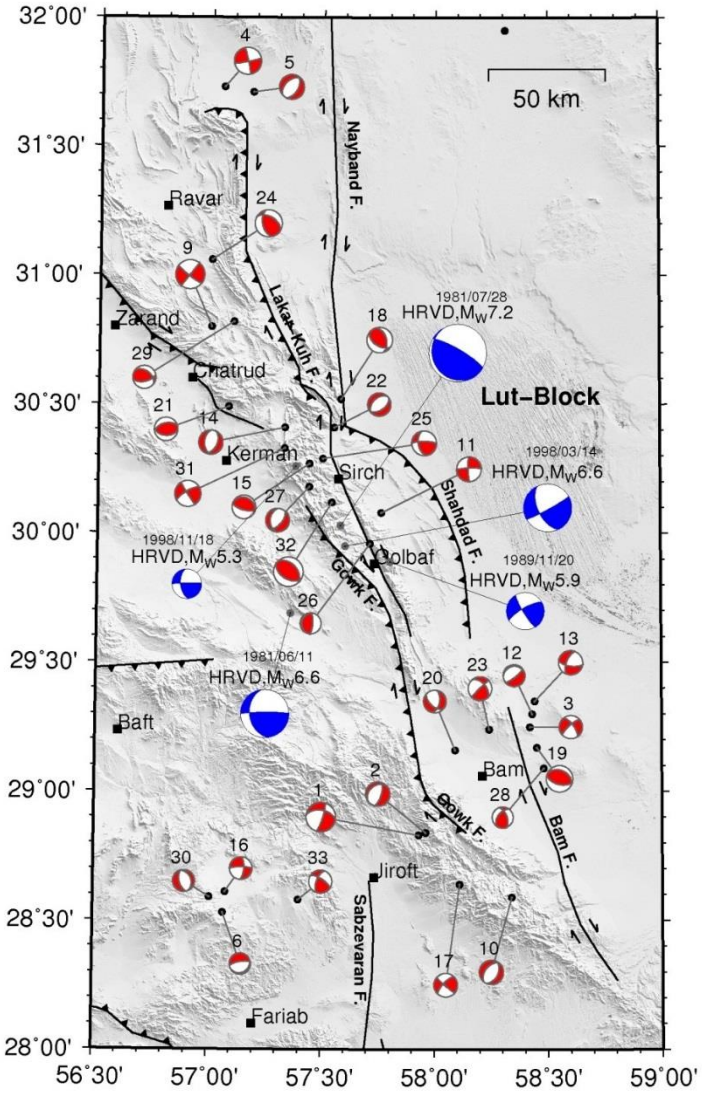

Fig. 4. The 32 focal mechanisms (the beachballs show the double couple part of the CMT solutions) with their related locations derived from full waveform modeling. The size of each beachball is also related to its magnitude, except for the 5 blue ones by Global CMT which are the prime events happened in this region. The main mechanism is strike-slip and reverse. The solid lines show traces of active faults in the region (Hessami et al., 2003).

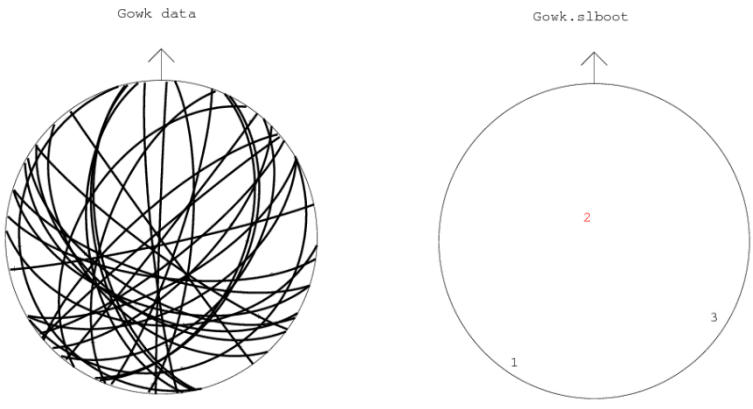

(a) **(b)**

Fig. 5. (a) Re-sampling of the 32 focal mechanisms; (b) The trend and plunge values of the three principal stress axes in the west Lut-Block; As it is clear, the second stress axis is nearly vertical.

Table 4. Source parameters of the 34 events in the region of study were calculated by the ISOLA software. The amounts of strike, dip and rake are for the double couple part of the CMT solutions. For events number 1 and 32 the source parameters calculated by Harvard CMT have also been shown.

No.	Date (y/m/d)	No. of Stations	Frequency	Centroid Depth	M_w	Var. Reduction	Dc%	System's Eigenvalue (min/max)	Strike (°)	Dip (°)	Rake (°)	Focal mechanism
1	2004/10/06	5	0.02-0.05	9	5	0.71	57.7	0.201	279 18	51 79	-14 -141	
CMT	2004/10/06			-	5.2	-	74	-	280 189	75 86	4 165	
2	2004/10/07	5	0.04-0.07	8	4.1	0.41	76	0.131	17 229	66 28	-105 -61	
3	2004/10/08	4	0.035-0.075	7	3.9	0.49	71.1	0.120	324 229	69 75	-164 -22	
4	2004/10/14	5	0.03-0.08	11	4.6	0.29	77.3	0.152	348 78	86 86	176 4	
5	2004/10/14	5	0.035-0.065	8	4.2	0.51	44.2	0.066	29 227	48 44	-102 -77	
6	2004/12/23	4	0.05-0.1	5	3.6	0.27	93.8	0.091	260 59	74 17	-84 -111	
7	2005/01/10	4	-	-	-	-	-	-	-	-	-	-
8	2005/01/30	5	-	-	-	-	-	-	-	-	-	-
9	2005/05/01	4	0.015-0.055	5	4.9	0.80	34.5	0.044	128 38	82 89	-179 -8	
10	2005/09/05	5	0.03-0.07	7	4.1	0.42	61.6	0.095	26 218	44 47	-99 -81	
11	2005/12/27	5	0.03-0.06	19	4.2	0.44	84.4	0.156	268 177	82 84	-174 -8	
12	2006/02/06	4	0.04-0.08	5	3.7	0.46	57.7	0.104	257 52	15 77	-65 -96	
13	2006/02/06	5	0.04-0.09	5	4.1	0.57	47.7	0.075	202 98	62 67	-153 -31	
14	2006/06/04	5	0.04-0.075	7	4.1	0.72	41.8	0.176	24 183	46 46	-75 -105	
15	2006/08/31	4	0.045-0.075	5	4	0.50	65.3	0.113	106 298	69 21	86 101	
16	2006/10/25	5	0.04-0.07	21	3.8	0.18	65.8	0.250	4 269	67 79	-168 -24	
17	2006/12/09	5	0.03-0.07	19	4	0.52	63.2	0.223	131 223	85 71	161 5	
18	2006/12/13	5	0.03-0.07	18	4.3	0.60	75.2	0.292	124 342	52 45	64 119	
19	2007/03/26	4	0.03-0.055	7	4.5	0.60	81.1	0.136	294 106	36 54	97 85	
20	2007/12/25	4	0.035-0.065	5	3.8	0.30	94.6	0.180	10 133	54 53	-48 -132	
21	2008/05/27	4	0.03-0.07	16	4	0.61	85.6	0.140	93 255	43 48	103 78	
22	2008/06/21	4	0.035-0.065	5	3.9	0.43	92.2	0.097	55 225	49 41	-84 -97	
23	2008/06/23	4	0.05-0.1	21	4	0.63	84.9	0.214	226 319	87 49	139 3	
24	2009/02/15	5	0.055-0.095	8	4.6	0.71	54.1	0.223	167 300	53 48	123 54	
25	2009/05/11	7	0.035-0.065	21	4.2	0.60	73.1	0.259	270 170	77 51	40 163	
26	2009/06/24	7	0.065-0.095	8	3.6	0.39	58.4	0.150	186 5	16 74	92 90	
27	2009/10/17	6	0.05-0.08	5	4	0.63	80.3	0.119	39 185	58 37	-70 -119	
28	2010/01/05	6	0.065-0.1	6	3.6	0.12	81.1	0.155	218 338	52 57	136 47	
29	2010/01/26	6	0.07-0.105	18	3.9	0.21	47.2	0.113	77 307	58 44	58 130	
30	2010/02/03	8	0.07-0.1	19	3.7	0.15	40.9	0.190	338 165	34 56	-96 -86	
31	2011/01/09	8	0.05-0.1	19	4.4	0.51	99.8	0.233	148 238	88 73	163 2	
32	2011/06/26	7	0.045-0.075	12	5	0.62	73.3	0.212	316 121	42 49	101 80	
CMT	2011/06/26		-	-	5.1	-	-	-	114 317	36 56	71 103	
33	2012/04/29	8	0.07-0.1	34	3.9	0.19	90	0.192	201 302	61 70	157 31	
34	2012/09/21	8	0.035-0.065	6	4.4	0.50	95.8	0.138	134 331	56 35	80 105	

6. Conclusions

According to the high seismicity in the Eastern part of Iran, especially around the Lut-Block, it is necessary to do more research in this area. In the mentioned area, we focused on the west part of Lut-Block for two reasons. First, the fault system here passes through dense-population towns. The second, this system has had a considerable activity in the past fifty years. To assess the seismic hazard in a region, the responsible faults and their main mechanisms, the focal mechanisms of the earthquakes, their magnitude and depth and other source parameters should be known. Hence, a great number of researches have been conducted in an effort to reach better and more precise methods to calculate the source parameters. In this regard, we tried to determine the source parameters of the earthquakes happened on the Gowk fault between 2004 and 2012 by means of moment tensor inversion using ISOLA software. What makes this method more powerful than others is that it uses the local and regional seismogram data, in that the data have more information of the source. We also compared two of the focal mechanisms with what had been stated before on Harvard CMT catalog (Table 4). As can be seen there is a correspondence between the results.

As Figure 4 shows the focal mechanism calculated for the most considerable events 1, 4, 9, 19, 24, 31, 32, and 34 (the red beach balls), is strike-slip and reverse. The published mechanism for the main events happened between 1981 and 1998 (the blue beach balls) shows the same mechanism. Nonetheless, it is evident that there are some other mechanisms that we calculated on this fault system. To investigate the variety of mechanisms occurred in this area it is helpful to consider the regional tectonics and local geomorphology. The Nayband-Gowk-Sabzevaran fault system is a long right-lateral strike-slip system bordering the western side of the Lut-Block. Both the Nayband and Sabzevaran faults are not associated with much topographic relief except near their junctions with the Gowk fault. By contrast, the Gowk fault is associated with substantial topographic relief. From this evidence, we expect the Gowk fault system to involve an overall component of shortening. This spatial separation of strike-slip and shortening components of oblique convergence is known as ‘partitioning’ (Berberian et al., 2001; McCaffrey, 1992). Therefore, as mentioned before in Figure 4 we can see some events with reverse mechanisms (e.g. 18, 21, 29 and 32) while some others are strike-slip (e.g. 9, 11, 25 and 31). It is also worth mentioning that the Gowk fault is in a clear pull-apart relation with the southern end of the Nayband fault because of its low elevation (Berberian et al., 2001). This is where we can observe the events 14 and 22 with normal mechanisms. It is probable to have the same pull-apart situation in the southern part of the Gowk fault; the place where there are some normal components (e.g. 1, 2 and 20). Thus, according to the 32 focal mechanisms determined in this study, the main mechanism on the Nayband-Gowk fault system is right-lateral strike-slip with a reverse component. However, it should not be forgotten that the occurrence of normal mechanisms is possible since there are some pull-apart basins. Finally, stress inversion applied to the 32 focal mechanisms and the three principal stress axes in the area was derived from the second one being nearly vertical which is characteristic of the strike-slip regions.

Acknowledgements

We thank International Institute of Earthquake Engineering and Seismology for supplying the waveform data. We would like to thank Professor Zahradnik for providing the ISOLA software. We also acknowledge Dr. Michael for the bootstrap code.

References

Berberian, M., Jackson, J., Fielding, E., Parsons, B., Priestley, K., Qorashi, M., Talebian, M., Walker, R., Wright, T. and Baker, C., 2001, The 1999 March 14 Fandoqa earthquake (Mw= 6.6) in Kerman province, southeast Iran: re-rupture of the 1981Sirch earthquake fault, triggering of slip on adjacent thrusts and the active tectonics of the Gowk fault zone, Geophys. J. Int., 146, 371-398.

Bott, M. H. P., 1959, The mechanics of oblique slip faulting, Geol. Mag., 96, 109-117.

Bouchon, M., 1981, A simple method to

calculate Green's functions for elastic layered media, Bull. Seismo. Soc. Am., 71, 959-971.

Dziewonski, A. M., Chou, T. A. and Woodhouse, J. H., 1981, Determination of earthquake source parameters from waveform data for studies of global and regional seismicity, J. Geophys. Res., 86, 2825-52.

Henry, C., Woodhouse, J. H. and Das, S., 2002, Stability of earthquake moment tensor inversions: effect of the double-couple constraint, Tectonophysics, 356, 115-124.

Hessami, K., Jamali, F. and Tabassi, H., 2003, Major active faults of Iran, scale 1:25,000,000, Ministry of Science, Research and Technology, International Institute of Earthquake Engineering and Seismology.

Kanamori, H. and Given, J. W., 1981, Use of long period surface waves for rapid determination of earthquake source parameters, Phys. Earth Planet. Inter., 27, 8-31.

Kikuchi, M. and Kanamori, H., 1991, Inversion of complex body waves-III, Bull. Seismol. Soc. Am., 81, 2335-2350.

McCaffrey, R., 1992, Oblique plate convergence, slip vectors, andforearc deformation, J. geophys. Res., 97, 8905-8915.

Michael, A. J., 1984, Determination of stress from slip data, faults and folds, J. Geophys. Res., 89, 11517-11526.

Michael, A. J., 1987, Use of focal mechanisms to determine stress: a control study, J. Geophys. Res., 92, 357-368.

Sokos, E. and Zahradnik, J., 2008, ISOLA a Fortran code and a Matlab GUI to perform multiple-point source inversion of seismic data, Computers and Geosciences, 34, 967-977.

Strelitz, R. A., 1978, Moment tensor inversions and source models, Geophys. J. Roy. Astron. Soc., 52, 359-64.

Walker, R. and Jackson, J., 2002, Offset and evolution of the Gowk fault, S. E. Iran: a major intra-continental strike-slip system, Journal of Structural Geology, 24, 1677-1698.

Walker, R., Jackson, J. and Baker, C., 2004, Active faulting and seismicity of the Dasht-e-Bayaz region, eastern Iran, Geophys. J. Int., 157, 265-282.

Zahradnik, J., Jansky, J. and Papatsimpa, K., 2001, Focal mechanisms of weak earthquakes from amplitude spectra and polarities, Pure appl. Geophys., 158, 647-665.

Zahradnik, J., Jansky, J. and Plicka, V., 2008, Detailed waveform inversion for moment tensors of M~ 4 events: examples from the Corinth Gulf, Greece, Bull. Seismol. Soc. Am., 98, 2756-2771.

Zahradnik, J., Serpetsidaki, A., Sokos, E. and Tselentis, G. A., 2005, Iterative deconvolution of regional waveforms and double-event interpretation of 2003 Lefkada earthquake, Greece, Bull. Seismol. Soc. Am., 95,159-172.